



City Research Online

City, University of London Institutional Repository

Citation: Baronchelli, A., Catanzaro, M. & Pastor-Satorras, R. (2008). Random walks on complex trees. *Physical Review E (PRE)*, 78(1), 011114. doi: 10.1103/physreve.78.011114

This is the accepted version of the paper.

This version of the publication may differ from the final published version.

Permanent repository link: <https://openaccess.city.ac.uk/id/eprint/13936/>

Link to published version: <https://doi.org/10.1103/physreve.78.011114>

Copyright: City Research Online aims to make research outputs of City, University of London available to a wider audience. Copyright and Moral Rights remain with the author(s) and/or copyright holders. URLs from City Research Online may be freely distributed and linked to.

Reuse: Copies of full items can be used for personal research or study, educational, or not-for-profit purposes without prior permission or charge. Provided that the authors, title and full bibliographic details are credited, a hyperlink and/or URL is given for the original metadata page and the content is not changed in any way.

Random walks on complex trees

Andrea Baronchelli, Michele Catanzaro, and Romualdo Pastor-Satorras

Departament de Física i Enginyeria Nuclear, Universitat Politècnica de Catalunya, Campus Nord B4, 08034 Barcelona, Spain

(Dated: February 19, 2013)

We study the properties of random walks on complex trees. We observe that the absence of loops reflects in physical observables showing large differences with respect to their looped counterparts. First, both the vertex discovery rate and the mean topological displacement from the origin present a considerable slowing down in the tree case. Second, the mean first passage time (MFPT) displays a logarithmic degree dependence, in contrast to the inverse degree shape exhibited in looped networks. This deviation can be ascribed to the dominance of source-target topological distance in trees. To show this, we study the distance dependence of a symmetrized MFPT and derive its logarithmic profile, obtaining good agreement with simulation results. These unique properties shed light on the recently reported anomalies observed in diffusive dynamical systems on trees.

PACS numbers: 89.75.Hc, 05.40.Fb, 05.60.Cd

I. INTRODUCTION

Diffusion problems on tree structures pop up in a wide range of scientific domains, such as theoretical physics [1, 2, 3], computer science [4, 5], phylogenetic analysis [6] and cognitive science [7]. Moreover, dynamics in tree structures have gained a renewed interest in the physics community as a spin-off of the attention devoted to the structural properties of complex networks [8, 9] and dynamical processes taking place on top of them [10]. Thus, along with the widely explored scale-free (SF) networks [11], also SF trees have started to be used as underlying topologies for dynamical processes. Interestingly, the absence of loops in trees turns out to have a strong impact on the considered dynamics, and relevant differences between looped networks and tree topologies have been recently reported in several dynamical models, such as the voter model [12], the naming game [13], the random walk and the pair-annihilation processes [14], and a model for norm spreading [15]. The properties of most dynamical processes on looped network can be reasonably accounted for by annealed mean-field theories [10], which rely only on information about the degree distribution and degree correlations [16], and consider the network as maximally random at all other respects. The behavior observed in trees, different from the annealed mean-field predictions, must thus be explained in terms of the non-local constrain of absence of loops imposed in this kind of graphs, which is hard to implement in theoretical approaches.

In this paper we explore the peculiarities induced in dynamical processes by the absence of loops by considering the simplest possible example, namely the uncorrelated random walk [17, 18]. Several works have been devoted in the past to the study of random walks on complex networks, showing in general a good agreement between theory and simulations on looped networks, while differences were reported in tree networks in Ref. [14]. Here, we find that the global constraint of lack of loops induces a general slowing down of diffusion, as measured by the network coverage and the mean topological displacement

from the origin. As well, it profoundly alters the degree dependence of the mean-first passage time. This is due to the fact that the source-target distance is dominating in trees. In order to account for this features, we study the mean round trip time versus distance and find an analytic expression of its dependence on degree.

II. RANDOM WALKS ON COMPLEX NETWORKS AND TREES

We consider random walks on general networks defined by a walker that, located on a given vertex of degree k at time t , hops with probability $1/k$ to one of the k neighbors of that vertex at time $t + 1$. We have measured the properties of random walks on growing SF trees created with the linear preferential attachment (LPA) algorithm [11, 19]: at each time step s , a new vertex with m edges is added to the network and connected to an existing vertex s' of degree $k_{s'}$ with probability $\Pi_{s \rightarrow s'} = (k_{s'} + a)/(2m + a)s$. This process is iterated until reaching the desired size N . The resulting network has degree distribution $P(k) \sim k^{-\gamma}$ with tunable exponent $\gamma = 3 + a/m$, with $\gamma < 3$ for $a < 0$. For $m = 1$ the LPA model yields a strict tree topology. Degree correlations, measured by the average degree of the nearest neighbors of the vertices of degree k [20], are given by $\bar{k}_{nn}(k) \sim N^{(3-\gamma)/(\gamma-1)}k^{-3+\gamma}$ [21]. Therefore, only for $\gamma = 3$ ($a = 0$) we expect to obtain uncorrelated networks.

In order to explore the intrinsic properties of a tree topology, disregarding SF effects, we have also considered homogeneous networks. In the growing exponential network model (EM) [9], at each time step s a new vertex with m edges is added to the network, and it is connected to m randomly chosen other vertices. In the continuous degree approximation (i.e., considering the degree as a continuous variable and substituting sums by integrals), this models leads to networks with an exponential degree distribution, $P(k) = e^{1-k/m}/m$. Again, homogeneous trees are generated by selecting $m = 1$. The random Cayley tree (RC), on the other hand, is generated by

adding z neighbors to a randomly selected leaf (i.e. a vertex whose degree is $k = 1$) at each time step s ($z + 1$ neighbors are added to the first vertex). The resulting tree contains only vertices with degree $k = z + 1$, and leaves with $k = 1$.

To check our results against looped structures, we have considered the uncorrelated configuration model (UCM) [22], yielding uncorrelated networks with any prescribed SF degree distribution. The model is defined as follows: (1) Assign to each vertex i in a set of N initially disconnected vertices a degree k_i , extracted from the probability distribution $P(k) \sim k^{-\gamma}$, and subject to the constraints $m \leq k_i \leq N^{1/2}$ and $\sum_i k_i$ even. (2) Construct the network by randomly connecting the vertices with $\sum_i k_i/2$ edges, respecting the preassigned degrees and avoiding multiple and self-connections. Using this algorithm, it is possible to create SF networks which are completely uncorrelated. Additionally, by selecting the minimum degree $m \geq 2$, we generate connected networks with probability almost 1. The effect of correlations in looped structures can be checked by means of the configuration model (CM) [9], which is analogous to the UCM, but allows degrees to range in the interval $m \leq k_i \leq N$ [23]. In all present simulations, we set for looped networks $m = 4$, tree networks corresponding to $m = 1$ ($z = 4$ for the RC tree).

III. RANDOM WALK EXPLORATION

We start by studying two properties of a random walk that quantify the speed at which it explores its neighborhood in the network. The first one is the coverage $S(t)$, defined as the number of different vertices visited by a walker at time t , averaged for different random walks starting from different sources. For looped networks, the coverage reaches after a short transient the functional form [24, 25] $S_L(t) \sim t$ [43], in accordance with theoretical calculations for the Bethe lattice [26], and eventually saturates to $S_L(\infty) = N$, due to finite size effects. A scaling form for the coverage has been proposed [24] to be $S_L(t) = Nf(t/N)$, with $f(x) \sim x$ for $x \ll 1$ and $f(x) \sim 1$ for $x \gg 1$.

The origin of the scaling of the coverage with system size can be understood by means of a simple dynamic mean-field argument. Let us define $\rho_k(t)$ as the probability that a vertex of degree k hosts the random walker at time t . During the evolution of the random walk, this probability satisfies, in a general network with a correlation pattern given by the conditional probability $P(k'|k)$ that a vertex of degree k is connected to another vertex of degree k' [16], the mean-field equation

$$\frac{\partial \rho_k(t)}{\partial t} = -\rho_k(t) + k \sum_{k'} \frac{P(k'|k)}{k'} \rho_{k'}(t). \quad (1)$$

In the steady state, $\partial_t \rho_k(t) = 0$, the solution of this equation, for any correlation pattern, is given by the normal-

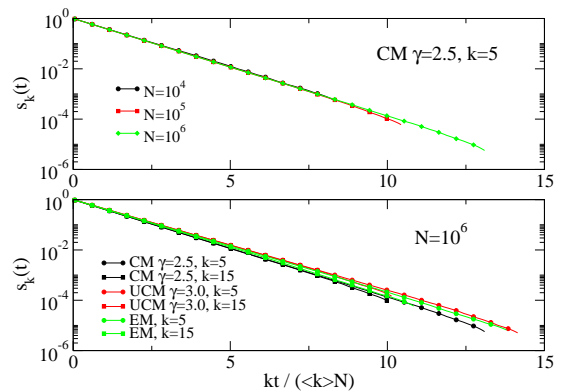


FIG. 1: (Color online) Coverage spectrum $s_k(t)$ in looped complex networks as a function of $kt/\langle k \rangle N$. Top: Curves for the same degree and different network size N . Bottom: Curves for different degrees and fixed network size.

ized distribution [18, 27]

$$\rho_k(t) = \frac{k}{\langle k \rangle N}. \quad (2)$$

Let us now define the coverage spectrum $s_k(t)$ as fraction of vertices of degree k visited by the random walker at least once. Obviously, we have that $S(t) = N \sum_k P(k) s_k(t)$. The spectrum $s_k(t)$ increases in time as the random walk arrives to vertices that have never been visited. Therefore, at a mean-field level, it fulfills the rate equation

$$\frac{\partial s_k(t)}{\partial t} = k[1 - s_k(t)] \sum_{k'} \frac{P(k'|k)}{k'} \rho_{k'}(t). \quad (3)$$

Approximating $\rho_{k'}(t)$ by its steady-state value (for not too small times), we obtain

$$\frac{\partial s_k(t)}{\partial t} = [1 - s_k(t)] \frac{k}{\langle k \rangle N}, \quad (4)$$

whose solution, with the initial condition $s_k(0) = 0$ is

$$s_k(t) = 1 - \exp\left(-\frac{kt}{\langle k \rangle N}\right). \quad (5)$$

We therefore are lead to the general scaling expression

$$\frac{S(t)}{N} = 1 - \sum_k P(k) \exp\left(-\frac{kt}{\langle k \rangle N}\right). \quad (6)$$

In the limit of $kt/\langle k \rangle N \ll 1$, we recover the exact result $S(t) \sim t$ [26]. For SF networks, we obtain within the continuous degree approximation

$$\begin{aligned} \frac{S(t)}{N} &= 1 - (\gamma - 1) m^{\gamma-1} \int_m^\infty k^{-\gamma} \exp\left(-\frac{kt}{\langle k \rangle N}\right) dk \\ &= 1 - (\gamma - 1) E_\gamma\left(\frac{mt}{\langle k \rangle N}\right), \end{aligned} \quad (7)$$

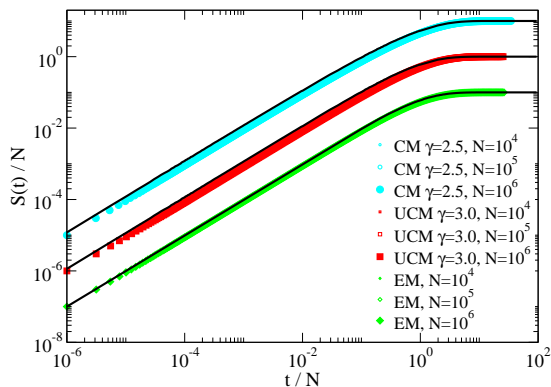


FIG. 2: (Color online) Rescaled coverage for looped complex networks. We plot in full lines the analytical predictions Eqs. (7) and (8), corresponding to SF and EM networks. Results for CM, UCM, and EM networks have been shifted (top to bottom) in the vertical axis for clarity.

where $E_\gamma(z)$ is the exponential integral function [28]. For EM networks, on the other hand, we find

$$\begin{aligned} \frac{S(t)}{N} &= 1 - \frac{e}{m} \int_m^\infty e^{-k/m} \exp\left(-\frac{kt}{\langle k \rangle N}\right) dk \\ &= 1 - \frac{e^{-mt/\langle k \rangle N}}{1 + \frac{mt}{\langle k \rangle N}}. \end{aligned} \quad (8)$$

In Fig. 1, we can observe that the scaling predicted by Eq. (5) for the coverage spectrum $s_k(t)$ is very well satisfied in looped complex networks, independently of their homogeneous or SF nature, and in this last case, of the degree exponent and the presence or absence of correlations. In Fig. 2, on the other hand, we plot the total coverage $S(t)/N$, which can be fitted quite correctly by the analytical expressions Eqs. (7) and (8) for SF and EM networks.

On tree networks we find a different scenario. In Fig. 3 we can see that the coverage spectrum does not scale as predicted by our mean-field argument. While we do not have theoretical predictions for the correct scaling form, a numerical analysis of the total coverage, Fig. 4, shows that, at short times, it grows in trees as $S_T(t) \sim t/\ln(t)$, preserving an approximate scaling form

$$S_T(t) = Nf\left(\frac{t}{\ln(t)N}\right), \quad (9)$$

with a scaling function $f(x)$ that depends slightly on the network details (degree exponent, correlations, etc.). This observation indicates the presence of a general slowing down mechanism in the random walk dynamics in trees: the dynamics turns out to be more recurrent and therefore it is more costly to find new vertices during the walk. It is easy to see that this situation will correspond to a walker deep in the leaves of a subtree that has otherwise completely explored. In order to find new vertices, the walker must first find the exit to the subtree. This

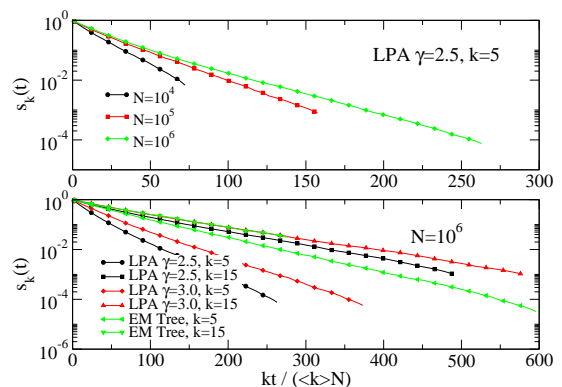


FIG. 3: (Color online) Coverage spectrum $s_k(t)$ in tree networks as a function of $kt/\langle k \rangle N$. Top: Curves for the same degree and different network size N . Bottom: Curves for different degrees and fixed network size. The scaling here is different from the mean-field prediction Eq. (5).

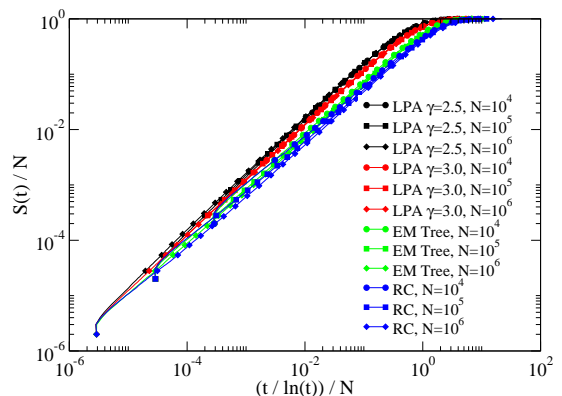


FIG. 4: (Color online) Rescaled coverage as a function of time in complex trees. Results for LPA ($\gamma = 2.5$), LPA ($\gamma = 3.0$), EM, and RC networks have been shifted (top to bottom) in the vertical axis for clarity.

difficulty in finding new vertices can be directly measured by the time lag Δt between the discovery of two new vertices. In Fig. 5 we plot the probability distribution of time lags, $P(\Delta t)$, computed for the discovery of the first 1% of the network, for looped and tree structures. We observe that, in looped networks, this distribution takes an exponential form, compatible with an almost constant time lag between the discovery of two new vertices. In tree networks, this distribution shows instead long tails, that can be fitted to a lognormal form, indicating that, in some events (i.e. when the walker is trapped in one leaf in a subtree) the discovery of a new vertex can take an unusually large time.

Acute signatures of slowing down can be found also in the analysis of the mean topological displacement (MTD) $\bar{d}(t)$ of the walker from its origin at time t , defined as the shortest path length from the vertex of origin of the random walk, to the vertex it occupies at time t , averaged over different source vertices, and different random walk

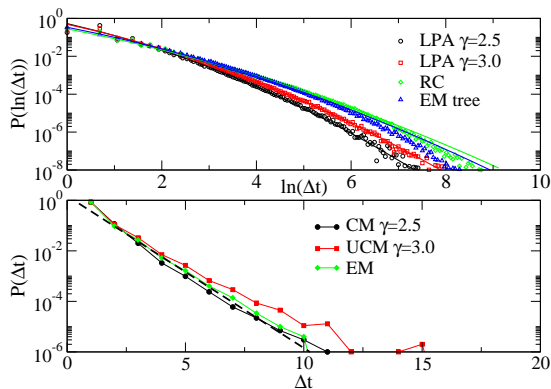


FIG. 5: (Color online) Distribution of lag times in tree (top) and looped (bottom) networks can be fitted, respectively, by a log-normal (full lines) and an exponential (dashed line) distribution. Data refer to graphs of size $N = 10^5$.

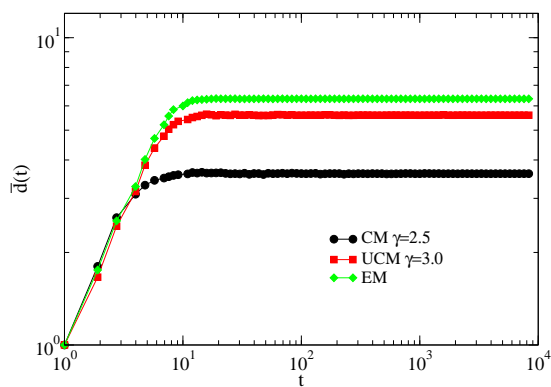


FIG. 6: (Color online) MTD as a function of time for looped complex networks of size $N = 10^6$.

realizations. In other works, the mean square topological displacement (RMSTD) $\bar{d}^2(t)$ [25, 29] was instead considered. In complex networks, and since the shortest path length is a positive definite quantity, both quantities yield the same scaling result, i.e. $\bar{d}^2(t) \sim [\bar{d}(t)]^2$ [44].

In looped networks, see Fig. 6, we observe a very rapid increase of the MTD with time. In previous works [29], the growth of the average distance (there measured instead as the RMSTD) was found to be a power law, $\bar{d}(t) \sim t^\alpha$ at early times in SF networks, with the exponent α depending on the degree exponent. In our simulations on looped networks generated with different algorithms, we do not find a clear signature for a power law behavior, which can only be approximately found in a tiny range of values of t at the very beginning of the walk, even for networks of size $N = 10^6$. At large times, on the other hand, the MTD reaches a plateau, $\bar{d}(\infty) = \langle \bar{d} \rangle$, due to finite size effects. The value of this plateau can be estimated using simple quantitative arguments. Assume that the random walker starts from a source vertex of degree k . During its dynamics in the steady state, it visits vertices of degree k' with probability, see Eq. (2), $k'/\langle k \rangle N$. On the other hand, vertices of

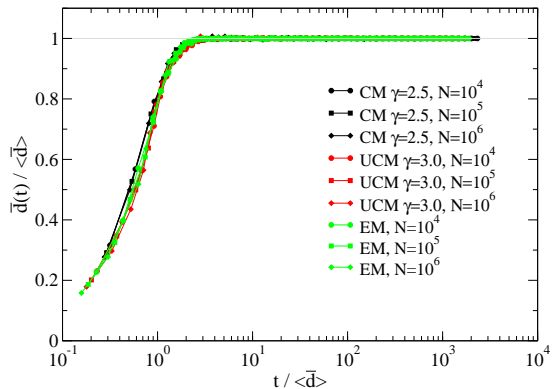


FIG. 7: (Color online) Rescaled MTD as a function of time for looped complex networks.

degree k and k' are, in average, at a topological distance [30, 31] $d_{k,k'}$; therefore, we will expect the random walker to be at an average distance of a source of degree k

$$\langle \bar{d} \rangle_k = \sum_{k'} \frac{k' P(k')}{\langle k \rangle} d_{k,k'}. \quad (10)$$

A further average over all possible sources, leads to an average distance of the walker, for any source vertex, given by

$$\langle \bar{d} \rangle = \sum_k P(k) \langle \bar{d} \rangle_k = \sum_k \frac{k P(k)}{\langle k \rangle} d_k, \quad (11)$$

where $d_k = \sum_{k'} P(k') d_{k,k'}$ is the mean topological distance from any vertex to a given vertex of degree k [31]. The scaling of $\langle \bar{d} \rangle$ with system size can be easily predicted assuming the expressions of d_k in Ref. [31], namely

$$d_k \simeq A \ln \left(\frac{N}{k^{(\gamma-1)/2}} \right) \quad (\text{SF networks}) \quad (12)$$

$$d_k \simeq A' \ln N - B' k \quad (\text{exponential networks}), \quad (13)$$

where A , A' and B' are size-independent constants. This yields in both cases

$$\langle \bar{d} \rangle \simeq \ln N. \quad (14)$$

Turning to the numerical data for looped networks in Fig. 7, we observe that it is compatible with a scaling behavior of the form

$$\bar{d}_L(t) = \langle \bar{d} \rangle f \left(\frac{t}{\langle \bar{d} \rangle} \right). \quad (15)$$

This scaling indicates that, after a short characteristic time $t_c \sim \langle \bar{d} \rangle \sim \ln N$, the walker is in average as far as the origin as it can be, and it can therefore freely explore the whole network.

In trees, Fig. 8, on the other hand, we observe a much slower growth of the MTD at early times, which can be approximately fitted with the form

$$\bar{d}_T(t) \sim (\ln t)^\alpha, \quad (16)$$

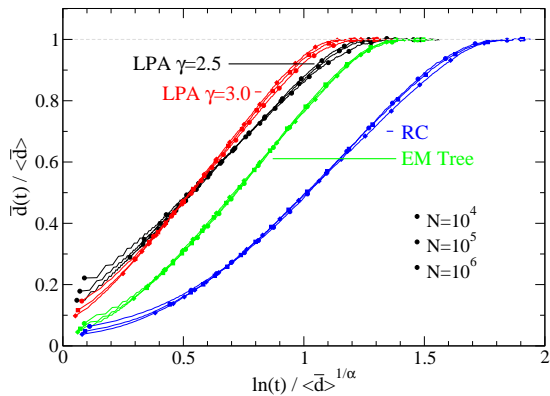


FIG. 8: (Color online) MTD as a function of time for complex trees of size $N = 10^6$. The exponent α is determined by a numerical fit from the observed relation $\bar{d}_T(t) \sim (\ln t)^\alpha$ (data not shown). The values used in Figure are $\alpha \simeq 0.91$ for LPA trees with $\gamma = 2.5$, $\alpha \simeq 1.04$ for LPA trees with $\gamma = 3.0$, $\alpha \simeq 1.31$ for EM trees and $\alpha \simeq 1.62$ for the RC tree.

where the exponent α depends on the details of the network. The whole function $\bar{d}_T(t)$ is also observed to fulfill the scaling form

$$\bar{d}_T(t) = \langle \bar{d} \rangle f \left(\frac{\ln t}{\langle \bar{d} \rangle^{1/\alpha}} \right). \quad (17)$$

This form implies that the characteristic time to escape from the neighborhood of the origin scales as $t_c \sim \exp(\langle d \rangle^{1/\alpha}) \sim \exp[(\ln N)^{1/\alpha}]$, which means that the exploration process is much more slower in trees, with the walker spending large amounts of time exploring the close vicinity of the origin of the walk. We remark that here the scaling function $f(x)$ displays some further dependences on degree exponent, average degree and degree correlations in both looped and tree networks.

The fact that the presence of a tree-like structure slows down the distance explored by a random walker on a network, allows to interpret the results presented in Ref. [29], in particular the power-law behavior at initial times of $\bar{d}(t)$. In fact, in Ref. [29] the substrate for the random walk simulations were SF networks generated with the CM model with minimum degree $m = 1$. In this case, simulations were performed on the giant component. Apart from the possible effect of degree correlations for $\gamma < 3$, the point is that, for $m = 1$, traces of tree-like structure are still present in the network, in the form of chains of small degree vertices [32]. Thus, a remnant slowing down effect of the tree component is observed, see Fig. 9, leading to an MTD that, at short times, scales as $\bar{d}(t) \sim t^{0.55}$ for the data at $m = 1$ shown in this graph, in excellent agreement with the observation in [29], namely $\bar{d}^2(t) \sim t^{1.1}$ for the RMSTD.

A further remark concerns the relation between our results and the above mentioned analytical calculations for Bethe lattices [26], according to which these structures exhibit a behavior analogous to the one observed in looped networks. The apparent incongruity vanishes

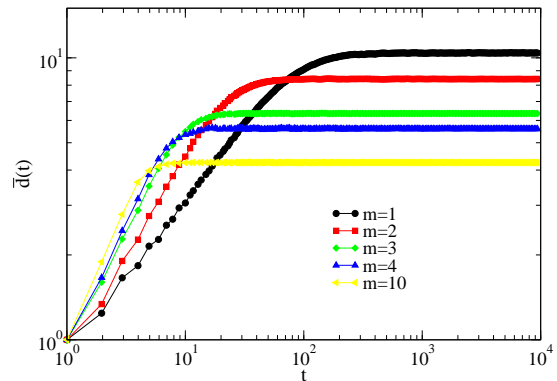


FIG. 9: (Color online) MTD as a function of time for UCM looped networks ($\gamma = 3.0$ and $N = 10^6$) with varying minimum degree m .

when noticing that, while Bethe lattices are infinite hierarchical structures, we have focused on complex (i.e. disordered) finite trees. To recover numerically the Bethe lattice behavior, indeed, it is necessary to adopt special algorithms in order to simulate an infinite hierarchical tree [33, 34].

IV. MEAN FIRST-PASSAGE TIME

More information about the dynamics of random walks can be extracted from the analysis of the mean first passage time (MFPT) [35] $\tau(i \rightarrow j)$, defined as the average time that a random walker takes to arrive for the first time at vertex j , starting from vertex i [27]. In networks with no translation symmetry, the MFPT from a source i to a target j needs not be equal to the MFPT from source j to target i . Therefore, different reduced MFPTs can be considered. We can thus define the direct MFPT $\tau^{\rightarrow}(k)$ as the MFPT on a target vertex of degree k , starting from a randomly chosen source vertex, and the inverse MFPT $\tau^{\leftarrow}(k)$ as the MFPT on a randomly target vertex, starting from a source vertex of degree k , namely

$$\tau^{\rightarrow}(k) = \frac{1}{N} \sum_i \frac{1}{N_k} \sum_{j \in \mathcal{V}(k)} \tau(i \rightarrow j), \quad (18)$$

$$\tau^{\leftarrow}(k) = \frac{1}{N} \sum_j \frac{1}{N_k} \sum_{i \in \mathcal{V}(k)} \tau(i \rightarrow j), \quad (19)$$

where $\mathcal{V}(k)$ is the set of vertices of degree k and N_k is the number of such vertices. A simple argument can predict the form of the MFPTs for random uncorrelated networks. In this case, the probability for the walker to arrive at a vertex i , in a hop following a randomly chosen edge, is given by $q(i) = q(k_i) = k_i / \langle k \rangle N$ [36]. Therefore, the probability of arriving at vertex i for the first time after t hops is $P_a(i; t) = [1 - q(i)]^{t-1} q(i)$. The direct

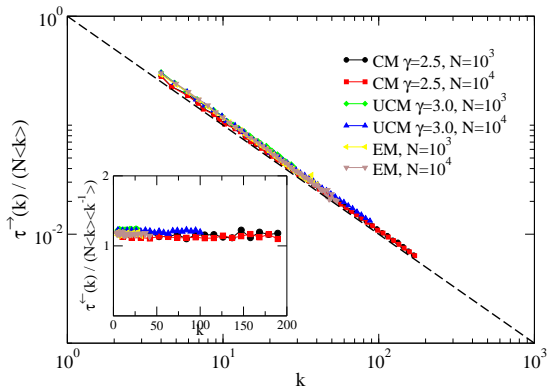


FIG. 10: (Color online) Reduced MFPTs as a function of the degree k for looped complex networks. We recover the simple mean-field predictions $\tau_L^{\rightarrow}(k) \simeq \langle k \rangle N/k$ (main figure) and $\tau_L^{\leftarrow}(k) \simeq \langle k \rangle \langle k^{-1} \rangle N$ (inset).

MFPT to vertex i can thus be estimated as the average

$$\tau^{\rightarrow}(k_i) = \sum_t t P_a(i; t) = \frac{\langle k \rangle N}{k_i}. \quad (20)$$

For the inverse MFPT, we notice that, in a random network, after the first hop, the walker loses completely the memory of its source degree, therefore we can approximate

$$\tau^{\leftarrow}(k) = \sum_k P(k) \tau^{\rightarrow}(k) = \langle k \rangle \langle k^{-1} \rangle N. \quad (21)$$

Less trivial approaches [27, 37] show in fact that the MFPT from a source vertex i to target vertex j depends on the degree of the target vertex as $\tau(i \rightarrow j) \sim 1/k_j$, but has a residual dependence on the source vertex and it is actually asymmetric, $\tau(i \rightarrow j) \neq \tau(j \rightarrow i)$. This fact could in principle affect the form of the reduced MFPTs in real networks, defined in Eqs. (18) and (19). Fig. 10, however, shows that for looped networks the behavior predicted for random uncorrelated networks turns out to be extremely robust with respect to changes in the topological properties of the network: homogeneous or heterogeneous nature, degree exponent, presence or absence of correlations, etc. [29, 37, 38].

In trees, on the other hand, we find a completely different picture, see Fig. 11. Now, the direct MFPT in SF trees decays with k much slower than in looped networks. In fact, we can fit it numerically to the form

$$\bar{\tau}_T^{\rightarrow}(k) = C_1 N \ln N - C_2 N \ln(k + C_3), \quad (22)$$

where C_1 , C_2 and C_3 fitting parameters that depend only slightly on the network size. The $N \ln N$ dependence can be directly observed by plotting $\bar{\tau}_T^{\rightarrow}(1)$ for different system sizes, as shown in Fig. 12. For homogeneous EM networks, on the other hand, the direct MFPT can be fitted to the form

$$\tau_T^{\rightarrow}(k) = D_1 N \ln N - D_2 N k, \quad (23)$$

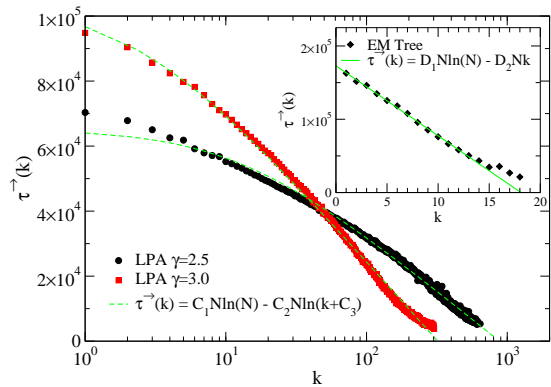


FIG. 11: (Color online) Direct MFPT as a function of the degree k for SF tree networks ($N = 10^4$). Dashed lines correspond to nonlinear fittings to the empirical form Eq. (22). Inset: Direct MFPT as a function of the degree k for homogeneous EM tree networks. The dashed line corresponds to a fitting to the empirical form Eq. (23).

see inset in Fig. 11. The scaling of $\bar{\tau}_T^{\rightarrow}(1)$ in this case is also checked in Fig. 12. With respect to the inverse MFPT, it is again constant, but now scales with system size as $\tau_T^{\leftarrow}(k) \sim N \ln N$ for all kinds of trees (inset in Fig. 12).

The topological structure of the trees can explain the unusual form of the MFPTs. While in looped networks the number of access paths to the target vertex is related to its degree, on the tree the path is unique, and is given by the one-dimensional set of links and vertices connecting the starting vertex to the target. In this case, the degree of the target is much less important from the point of view of the walker, since finding the target corresponds to finding a particular *leaf* (i.e. a $k = 1$ vertex) of the sub-tree the random walker is exploring. This observation suggests that while in looped networks the MFPT into a vertex is dominated by its degree (because the latter is related the multiplicity of the entry paths to the vertex), in trees the distance between the source and the target can be much more relevant, and thus induce a larger MFPT.

We therefore consider the MFPT as a function of the topological distance d_{ij} between the starting vertex i and the target j [37, 39]. Since the distance between two vertices is by definition a symmetric quantity, it seems natural to re-define the MFPT in terms of the symmetric mean round trip time (MRTT)

$$\bar{\tau}(d_{ij}) = \tau(i \rightarrow j) + \tau(j \rightarrow i), \quad (24)$$

i.e. the average time to go from i to j and back or vice-versa. It has been recently proved [39] that, for complex scale-invariant networks, the MRTT averaged for all vertices at the same distance scales as

$$\bar{\tau}(d) \simeq N d^{D_w - D_b}, \quad (25)$$

where D_b is the box dimension of the network, and D_w its walk exponent [40]. For a class of scale-invariant net-

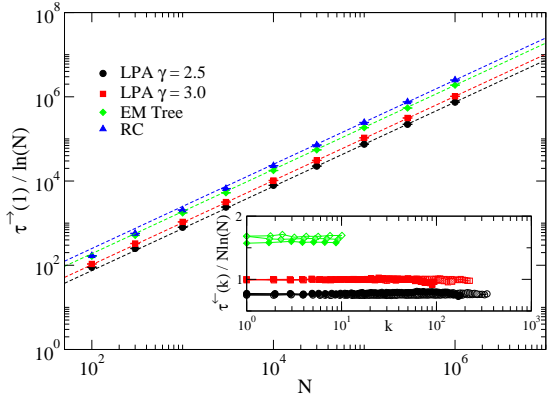


FIG. 12: (Color online) Direct MFPT on leaves in complex trees as a function of the network size N . The observed scaling is $\tau_T^-(1) \sim N \ln N$. Inset: Inverse MFPT on complex trees for different network sizes ($N = 10^3$ full colored points, $N = 3 \times 10^3$ light colored points, $N = 10^4$ empty points). The observed scaling is again $\tau_T^-(k) \sim N \ln N$.

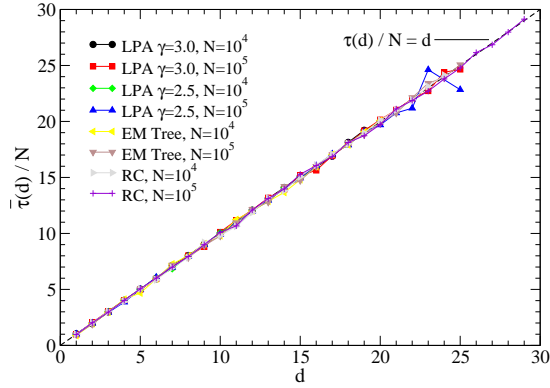


FIG. 13: (Color online) MRTT $\bar{\tau}_T(d)$ as a function of the source-target topological distance d in trees. Different curves collapse perfectly on $\bar{\tau}_T(d) \sim Nd$.

works [40] corresponding to a tree structure, for which $D_w - D_b = 1$, the authors of Ref. [39] obtained correspondingly a linear scaling $\bar{\tau}_T(d) \simeq Nd$. We have checked that this linear form holds for different SF, EM and RC trees, see Fig. 13, a result that leads us to conjecture that, for any complex tree, $D_w - D_b = 1$.

We can use the result in Eq. (25) to gain insight on the behavior of the anomalous reduced MFPTs in tree networks. Considering an average over all vertices with the same degree, we have that $\bar{\tau}(d_{kk'}) = \tau(k \rightarrow k') + \tau(k' \rightarrow k)$. Averaging now over k' , we can consider the reduced MRTT

$$\bar{\tau}(k) = \sum_{k'} P(k') [\tau(k \rightarrow k') + \tau(k' \rightarrow k)] = \tau_T^-(k) + \tau_T^+(k), \quad (26)$$

defined as the average time to go from a randomly chosen vertex to a given vertex of degree k , and back (or vice-versa, since the MRTT is symmetric). Now, since $\bar{\tau}(d_{kk'})$

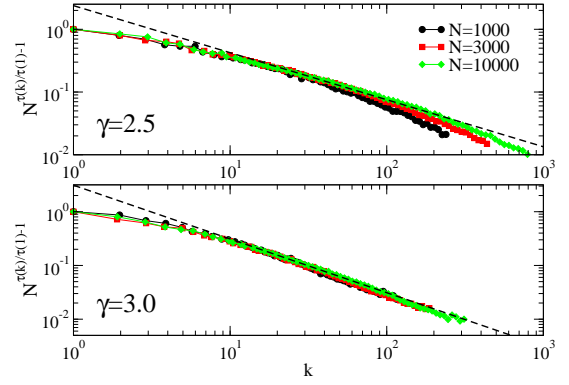


FIG. 14: (Color online) Rescaled MRTT $\bar{\tau}_T(t)$ as a function of the source degree k and for randomly chosen targets in SF trees. Predictions of Eq. (30), i.e. $N \bar{\tau}_T(k) / \tau_T^-(1) \sim k^{(1-\gamma)/2}$, are plotted as dashed lines.

is linear in $d_{kk'}$ for tree networks, we have

$$\bar{\tau}(k) \simeq \sum_{k'} P(k') N d_{kk'} = N d_k. \quad (27)$$

Assuming the scaling of d_k as given by Eqs. (12) and (13), we obtain

$$\bar{\tau}_T(k) \simeq N A \ln \left(\frac{N}{k^{(\gamma-1)/2}} \right) \quad (28)$$

for SF networks and

$$\bar{\tau}_T(k) \simeq N (A' \ln N - B' k) \quad (29)$$

for EM networks. The unknown constant in Eq. (28) can be reabsorbed in the value of $\bar{\tau}_T(1)$, to obtain a scaling form with system size for SF networks that reads

$$\frac{\bar{\tau}_T(k)}{\bar{\tau}_T(1)} \sim \frac{1}{\ln N} \ln \left(\frac{N}{k^{(\gamma-1)/2}} \right). \quad (30)$$

In Fig. 14 we show that this scaling form is very well satisfied by the MRTT in SF trees, independently of the degree exponent and correlation patterns, at least for intermediate values of k . The observed bending at small degrees can be ascribed to the presence of a constant in the logarithm analogous to empirical parameter C_3 in Eq. (22), that does not follow from our argument. Finite size effects, on the other hand, are responsible for the deviations present at large degrees, that are indeed more evident in SF trees with smaller values of γ .

This observations allow us to interpret the anomalous functional form of the reduced MFPTs observed in trees. From Eq. (26), we have

$$\tau_T^+(k) = \bar{\tau}_T(k) - \tau_T^-(k). \quad (31)$$

Writing $\tau_T^-(k) \sim CN \ln N$, from Eq. (28) we obtain, for SF networks,

$$\tau_T^+(k) \sim (A - C) N \ln N - \frac{A(\gamma - 1)}{2} N \ln k \quad (32)$$

while for homogeneous EM networks, we have

$$\tau_T^{\rightarrow}(k) \sim (A' - C)N \ln N - B'Nk, \quad (33)$$

in agreement with the empirical fitting found in Eqs. (22) and (23).

This argument cannot be extended to looped networks, since here $\bar{\tau}(d_{kk'})$ is not linear in $d_{kk'}$. The k dependence of the MRTT can be however trivially obtained from the reduced MFPTs as $\bar{\tau}_L(k) = \tau_L^{\rightarrow}(k) + \tau_L^{\leftarrow}(k) \simeq \langle k \rangle N (\langle k^{-1} \rangle + 1/k)$.

V. CONCLUSIONS

In this paper we have shown that complex tree-like topologies heavily affect the behavior of a random walk performed on top of them, with a global slowing down of the dynamics and a logarithmic dependence of the first passage time properties in SF networks. These features are intrinsically connected with the complex tree structure and cannot be attributed to the mere presence of leaves, while they are radically different from the ones exhibited by Bethe lattices, i.e. infinite and hierarchical tree structures.

We have studied the random walk exploration properties and we have shown that complex trees induce a slower dynamics, compared to looped networks, for

both the coverage and the mean topological displacement problems. Moreover, by means of the analysis of the symmetrized MFPT (the MRTT), we have been able to recognize the different role played by the degree k of the target vertex in looped and tree structures. In the former, a larger degree corresponds to a larger number of access ways to the target vertex. In the latter, on the other hand, the target vertex is always seen as a leaf by the random walker, and its degree k affects the MFPT only through the dependence of the average distance d_k between it and the rest of the vertices. These results provide important insights into diffusion problems on trees, and help explaining the characteristic slow dynamics observed on diffusive processes taking place on top of tree networks [12, 13, 14]. Moreover, they are also interesting in the study of dynamics in real-world networks, in which the so-called border trees motifs [41] have been recently shown to be significantly present.

Acknowledgments

We acknowledge financial support from the Spanish MEC (FEDER), under project No. FIS2007-66485-C02-01, and additional support from the DURSI, Generalitat de Catalunya (Spain). M. C. acknowledges financial support from Universitat Politècnica de Catalunya.

-
- [1] B. Huberman and M. Kerszberg, *J. Phys. A: Math. Gen.* **18**, L331 (1985).
 - [2] C. P. Bachas and B. A. Huberman, *Phys. Rev. Lett.* **57**, 1965 (1986).
 - [3] P. Sibani and K. H. Hoffmann, *Phys. Rev. Lett.* **63**, 2853 (1989).
 - [4] E. Lee and D. Raymond, *Encyclopedia of Microcomputers* **11**, 101 (1993).
 - [5] S. Card, J. Mackinlay, and B. Schneiderman, *Readings in Information Visualization: Using Vision to Think* (Morgan Kaufmann, San Francisco, 1999).
 - [6] L. Cavalli-Sforza and A. Edwards, *Evolution* **21**, 550 (1967).
 - [7] D. Fisher, *Machine Learning* **2**, 139 (1987).
 - [8] R. Albert and A.-L. Barabási, *Rev. Mod. Phys.* **74**, 559 (2002).
 - [9] S. N. Dorogovtsev and J. F. F. Mendes, *Evolution of networks: From biological nets to the Internet and WWW* (Oxford University Press, Oxford, 2003).
 - [10] S. Dorogovtsev, A. Goltsev, and J. Mendes, *Critical phenomena in complex networks* (2007), e-print arXiv:0705.0010v2.
 - [11] A.-L. Barabási and R. Albert, *Science* **286**, 509 (1999).
 - [12] C. Castellano et al., *Phys. Rev. E* **71**, 066107 (2005).
 - [13] L. Dall'Asta, A. Baronchelli, A. Barrat, and V. Loreto, *Phys. Rev. E* **74**, 036105 (2006).
 - [14] J. D. Noh and S. W. Kim, *Journal of the Korean Physical Society* **48**, S202 (2006).
 - [15] M. Nakamaru and S. Levin, *Journal of Theoretical Biology* **230**, 57 (2004).
 - [16] M. A. Serrano, M. Boguñá, R. Pastor-Satorras, and A. Vespignani, in *Large scale structure and dynamics of complex networks: From information technology to finance and natural sciences*, edited by G. Caldarelli and A. Vespignani (World Scientific, Singapore, 2007), pp. 35–66.
 - [17] B. Hughes, *Random walks and random environments* (Clarendon Press, Oxford (UK), 1995).
 - [18] L. Lovász, in *Combinatorics, Paul Erdős is Eighty* (János Bolyai Mathematical Society, Budapest, 1996), p. 353.
 - [19] S. N. Dorogovtsev, J. F. F. Mendes, and A. N. Samukhin, *Phys. Rev. Lett.* **85**, 4633 (2000).
 - [20] R. Pastor-Satorras, A. Vázquez, and A. Vespignani, *Phys. Rev. Lett.* **87**, 258701 (2001).
 - [21] A. Barrat and R. Pastor-Satorras, *Phys. Rev. E* **71**, 36127 (2005).
 - [22] M. Catanzaro, M. Boguñá, and R. Pastor-Satorras, *Phys. Rev. E* **71**, 027103 (2005).
 - [23] M. Boguñá, R. Pastor-Satorras, and A. Vespignani, *Euro. Phys. J. B* **38**, 205 (2004).
 - [24] D. Stauffer and M. Sahimi, *Phys. Rev. E* **72**, 46128 (2005).
 - [25] E. Almaas, R. V. Kulkarni, and Stroud, *Phys. Rev. E* **68**, 056105 (2003).
 - [26] B. D. Hughes and M. Sahimi, *J. Stat. Mech.* **29**, 781 (1982).
 - [27] J. Noh and H. Rieger, *Phys. Rev. Lett.* **92**, 118701 (2004).
 - [28] M. Abramowitz and I. A. Stegun, *Handbook of mathe-*

- mathematical functions.* (Dover, New York, 1972).
- [29] L. K. Gallos, Phys. Rev. E **70**, 046116 (2004).
- [30] J. A. Holyst et al., Phys. Rev. E **72**, 026108 (2005).
- [31] S. N. Dorogovtsev, J. Mendes, and J. Oliveira, Phys. Rev. E **73**, 056122 (2006).
- [32] A. N. Samukhin, S. N. Dorogovtsev, and J. F. F. Mendes, Phys. Rev. E **77**, 036115 (2008).
- [33] P. Argyrakis and R. Kopelman, Chemical Physics **261**, 391 (2000).
- [34] D. Katsoulis, P. Argyrakis, A. Pimenov, and A. Vitukhnovsky, Chemical Physics **275**, 261 (2002).
- [35] S. Redner, *A Guide to First-Passage Processes* (Cambridge University Press, Cambridge (UK), 2001).
- [36] M. E. J. Newman, in *Handbook of Graphs and Networks: From the Genome to the Internet*, edited by S. Bornholdt and H. G. Schuster (Wiley-VCH, Berlin, 2003), pp. 35–68.
- [37] A. Baronchelli and V. Loreto, Phys. Rev. E **73**, 026103 (2006).
- [38] A. Vázquez, M. Boguñá, Y. Moreno, R. Pastor-Satorras, and A. Vespignani, Phys. Rev. E **67**, 046111 (2003).
- [39] S. Condamin, O. Bénichou, V. Tejedor, R. Voituriez, and J. Klafter, Nature **450**, 77 (2007).
- [40] C. Song, S. Havlin, and H. Makse, Nature Physics **2**, 275 (2006).
- [41] P. Villas Boas, F. A. Rodrigues, G. Travieso, and L. Costa, *Border trees of complex networks* (2007), eprint arXiv:0706.3403v1.
- [42] D. J. Watts and S. H. Strogatz, Nature **393**, 440 (1998).
- [43] In the following, the subscripts L and T will indicate looped and tree networks, respectively.
- [44] Differences can however appear in networks with and underlying metric space, such as the Watts-Strogatz network [42] for rewiring parameter $p \ll 1$, see Ref. [25].